RESEARCH ON ANALYSIS OF MULTIFRACTAL CORRELATION CHARACTERISTICS OF AIRCRAFT ECHOES AND CLASSIFICATION OF TARGETS IN SURVEILLANCE RADARS

Qiusheng Li[1, 2] * and Weixin Xie[1]

[1]Intelligent Information Institute, Shenzhen University, Shenzhen 518060, China

[2]School of Physics and Electronic Information, Gannan Normal University, Ganzhou 341000, China

Abstract—Multifractal correlation, which studies the spatial correlation characteristics of two points with different singularity indexes, is a generalization of multifractal single point statistic. This paper introduces multifractal correlation theory into the characteristic analysis of aircraft echoes from low-resolution surveillance radars, and discusses the application of multifractal correlation characteristics in target classification. Firstly, on basis of introducing multifractal correlation theory, the multifractal correlation characteristics of aircraft echoes from surveillance radars are analyzed in detail by means of the multifractal correlation analysis. Secondly, on basis of the foregoing analysis, several characteristic parameters of the echo multifractal correlation spectrum are defined, and the support vector machine (SVM) based on the defined characteristic parameters is taken as the classifier to classify different types of aircraft targets. Finally, real recorded aircraft echo data are adopted to do the classification experiments, and the experimental results validate the proposed method.

1. INTRODUCTION

Most of active surveillance radars adopt the conventional low-resolution radar system. If they can provide class information of a target while detecting it, there will be undoubtedly important practical significance. Aircraft are a kind of main targets surveilled by surveillance radars. On one hand, they have complex shapes

and are nonrigid, and their nonrigid vibration or attitude change relative to the radar will induce complicated nonlinear modulations on the echo amplitude and phase [1]; on the other hand, echo modulation induced by their rotating parts (such as the rotor, empennage, propeller, turbine fan, etc.), called jet engine modulation (JEM), is also a typical nonlinear modulation, which is embodied in the echo characteristics such as amplitude, phase, frequency, and polarization and is independent from target attitude if there is no LOS-sheltering, i.e., the rotating parts can be seen by the radar [1–3]. These kinds of nonlinear modulations reflect the complicated micro-motion modulation effects of various parts of aircraft and contain target attribute information such as geometric structure, material composition, etc. [4, 5]. Different types of aircraft often have different structures and rotating parts, and have different nonrigid vibration and JEM characteristics. Therefore, if these nonlinear modulation features which reflect the physical characteristics of an aircraft target can be extracted effectively, then they provide possibilities for aircraft target classification and recognition.

So far, most of the features extracted in methods concerning target classification with low-resolution radars are based on JEM effect, and proposed extraction methods for JEM features mainly contain the complex cepstrum method, autocorrelation method, AR (auto regression) model power spectrum method, SVD (singular value decomposition) eigenvalue decomposition method, etc. [6–10]. However, these methods are mainly concentrated on estimating the interval of adjacent spectrum lines, and they often require a higher pulse repetition frequency (PRF) and longer observation time. In the conventional low-resolution radar system, it is often difficult to meet the higher-PRF and longer-observation-time requirements, and therefore the estimation accuracy of these methods is often unsatisfactory, which restricts their applications in practical engineering. [11] adopts fractional Brownian motion (fBm) to model aircraft echo from the viewpoint of nonlinear analysis and on this basis, proposes a target classification method based on echo fractal Brownian dimensions, thus avoids this problem to some extent. Yet it is difficult to fully characterize the complex nature of an aircraft echo by using only a single fractal dimension. Therefore, [12–14] perform multifractal modeling, characteristic analysis, and feature extraction on simulated and real-recorded aircraft echo data from low-resolution radars by means of the multifractal analysis of measures, and put forward some classification methods based on multifractal features. In spite of this, multifractal theory only performs statistical analysis on the singularity index of an arbitrary point in geometry subsets of

a fractal object, and then determines the multifractal spectrum, while the measure on the fractal object is generated by a potential series process. What multifractal describes is just its macroscopic properties, and a microcosmic description is needed for understanding its inherent physical nature more deeply.

Multifractal correlation extends the multifractal single point statistical characteristics. What it analyzes is the multifractal two-point statistical characteristics, and it mainly examines the probability observing the two given singular indexes on two points with a distance of d in geometry subsets of a fractal object. Because it takes the spatial correlation of singularity indexes into consideration, it can provide more comprehensive self-similar information than multifractal. Menuveau and Chhabra [15], Lee and Halsey [16], and O'Neil and Meneveau [17] did research for multifractal correlation theory earliest and analyzed the correlation characteristics of turbulence in the multifractal space. Zhou et al. [18] analyzed the multifractal and its correlation characteristics of random binomial measure and studied the phase transition problem between different scaling regions consisting in multifractal correlation. Shadkhoo and Jafari [19], Hajian and Movahed [20] investigated the seismic data and sunspot activity by means of multifractal correlation analysis and got a better result. Guan et al. [21, 22] introduced multifractal correlation theory into the characteristic analysis of sea clutter and low-observable target detection in sea clutter. Based on the above analyses, this paper intends to analyze the multifractal correlation characteristics of real-recorded echo data from low-resolution surveillance radars and on this basis puts forward a multifractal-correlation-feature-based classification method for aircraft targets so as to identify different types of aircraft targets in condition of no compensation for airframe echo components.

2. THEORETICAL BASIS AND PARAMETER ESTIMATION FOR MULTIFRACTAL CORRELATION

Multifractal correlation is the generalization of multifractal, and the calculation of its descriptive parameters is closely correlated with the multifractal descriptive parameters, which is generally realized by statistic physics methods. In the following, multifractal theory and multifractal correlation theory will be briefly introduced from the viewpoint of statistic physics respectively.

2.1. Multifractal

What multifractal describes is the characteristics of different levels of a fractal object in its measured distribution. Therefore, one can divide the investigated object into several small regions, noting the total number of the regions and the size of a region with N and ε ($\varepsilon < 1$), respectively, and let the measured distribution probability of the fractal object in a small region be $P_i(\varepsilon)$. Generally, there are different measured distribution probabilities in different regions, and the probabilities can be expressed by different indexes σ, i.e., [23]

$$P_i(\varepsilon) \propto \varepsilon^{\sigma}, \quad i = 1, 2, \ldots, N, \tag{1}$$

where σ is called local fractal-dimension, or singular index, whose value reflects the size of the measured distribution probability in a small region. Obviously, if the values of σ for all the regions are the same, then the investigated object is a mono-fractal object; contrarily, if the values of σ for different regions are different, then the investigated object is a multifractal object. Construct a subset with small regions with the same σ and note the number of these small regions with $N_\sigma(\varepsilon)$, then one has [23]

$$N_\sigma(\varepsilon) \propto \varepsilon^{-f(\sigma)} \, (\varepsilon \to 0), \tag{2}$$

where $f(\sigma)$ denotes the fractal dimension of this subset. For large number of small regions, one need use an infinite series $f(\sigma)$ corresponding to different σ to represent the fractal dimensions of the whole fractal object; therefore, $f(\sigma)$ is called multifractal spectrum.

To calculate the multifractal spectrum, firstly one may define a partition function [24]

$$\Gamma(q, \varepsilon) = \sum_{i=1}^{N} P_i^q(\varepsilon) = \varepsilon^{\tau(q)}, \tag{3}$$

where $\tau(q)$ is called mass index and $q \in (-\infty, +\infty)$, but one can determine its range according to the actual circumstances. Assuming that $\mu_\varepsilon(x)$ is the measured distribution function of the fractal object in the scale ε, one can get the q-order statistical moment of this measured distribution [25]

$$M_\varepsilon(q) = \left\langle \mu_\varepsilon^q(x) \right\rangle \propto \varepsilon^{D_0 + \tau(q)} \, (\varepsilon \to 0), \tag{4}$$

where, D_0 is the simple fractal-dimension of the fractal object; $\langle \cdot \rangle$ denotes mathematical expectation. Therefore, $\tau(q)$ is also known as moment exponent. Eq. (6) can be rewritten as [26]

$$\Gamma(q, \varepsilon) = \sum_{i=1}^{N} P_i^q(\varepsilon) = \sum N(P) P^q, \tag{5}$$

i.e., one can calculate $\sum P_i^q(\varepsilon)$ through grading the regions according to their measured distribution probabilities, where $N(P)$ denotes the number of the regions with the same probability P. Substituting Eqs. (1) and (2) into (5), then (5) can be further expressed as [26]

$$\Gamma\left(q,\varepsilon\right) = \sum \varepsilon^{\sigma q - f(\sigma)} = \varepsilon^{\tau(q)}. \tag{6}$$

Rewrite the right equation of Eq. (6) as [26]

$$\sum \varepsilon^{\sigma q - f(\sigma) - \tau(q)} = 1 \tag{7}$$

Obviously, when $\varepsilon \to 0$, those items with $\sigma q - f(\sigma) - \tau(q) > 0$ will verge on zero, while those items with $\sigma q - f(\sigma) - \tau(q) < 0$ will be impossible. Otherwise, the sum will become infinite. Hence only those items with $\sigma q - f(\sigma) - \tau(q) = 0$ will be kept, i.e., [26]

$$f\left(\sigma\right) = \sigma q - \tau\left(q\right), \tag{8}$$

and σ can be obtained by the differential coefficient of $\tau(q)$ on q, i.e., [26]

$$\sigma = d\tau\left(q\right)/dq. \tag{9}$$

It can be seen from Eqs. (8) and (9) that the relationship among $\tau(q)$, q and $f(\sigma)$, σ is the Legendre Transform, i.e., one can get the multifractal spectrum $f(\sigma)$ by the Legendre Transform of $\tau(q)$ and q.

2.2. Multifractal Correlation

It can be known from the analysis of the previous section that what multifractal examines is one-point statistical characteristics of the measured distribution in geometry subsets of a fractal object, that multifractal correlation extends it to two-point statistical characteristics, and that it studies the probability $P_\varepsilon\left(\sigma', \sigma'', d\right)$ observing the two given singular indexes σ' and σ'' on two points with a distance of d in geometry subsets of the fractal object, where σ' and σ'' are defined in the same scale ε, and d satisfies $\varepsilon < d < 1$ (if d is smaller than ε, the two points will be thought of as one point).

Define multifractal correlation spectrum $\tilde{f}(\sigma', \sigma'', \omega)$ as [18]

$$P_\varepsilon\left(\sigma', \sigma'', d\right) \propto \varepsilon^{D_0 - \tilde{f}(\sigma', \sigma'', \omega)}, \tag{10}$$

where $\omega = \ln d / \ln \varepsilon$. To derive the relationship between $\tilde{f}(\sigma', \sigma'', \omega)$ and $f(\sigma)$, firstly one can generalize the moment function defined in Eq. (4) and define a spatial autocorrelation function for the measured distribution [17]

$$C_\varepsilon\left(q', q'', d\right) = \left\langle \mu_\varepsilon^{q'}\left(x\right) \cdot \mu_\varepsilon^{q''}\left(x + d\right) \right\rangle \propto \varepsilon^{D_0 + \tilde{\tau}(q', q'', \omega)} \left(\varepsilon \to 0\right), \quad (11)$$

where $\tilde{\tau}(q', q'', \omega)$ is known as correlation moment exponent. In evidence, $C_\varepsilon(q', q'', d)$ contains more spatial information than $M_\varepsilon(q)$. For the mathematical expectation shown by Eq. (11), one can derive the following formula [17]

$$\left\langle \mu_\varepsilon^{q'}(x) \cdot \mu_\varepsilon^{q''}(x+d) \right\rangle \propto \varepsilon^{\tau(q')+\tau(q'')+2D_0+\omega \min\{\phi(q',q''),1\}} \, (\varepsilon \to 0), \quad (12)$$

where,

$$\phi\left(q', q''\right) = \tau\left(q' + q''\right) - \tau\left(q'\right) - \tau\left(q''\right) - D_0. \quad (13)$$

Comparing Eq. (11) with (12), one can get

$$\tilde{\tau}\left(q', q'', \omega\right) = \tau\left(q'\right) + \tau\left(q''\right) + D_0 + \omega \min\left\{\phi\left(q', q''\right), 1\right\}. \quad (14)$$

It can be seen from Eq. (14) that when $\phi(q', q'') = 1$, the first-order derivative of $\tilde{\tau}(q', q'', \omega)$ has a sudden change, which means that the transition between Region I ($\phi(q', q'') < 1$) and Region II ($\phi(q', q'') > 1$) is not continuous. This is the first order phase transition of the scaling behavior in multifractal theory [27]. When $\phi(q', q'') < 1$, one has [18]

$$\begin{cases} \sigma' = \omega\sigma\left(q' + q''\right) + (1 - \omega)\sigma\left(q'\right) \\ \sigma'' = \omega\sigma\left(q' + q''\right) + (1 - \omega)\sigma\left(q''\right) \end{cases}, \quad (15)$$

while when $\phi(q', q'') > 1$, one has [18]

$$\begin{cases} \sigma' = \sigma\left(q'\right) \\ \sigma'' = \sigma\left(q''\right) \end{cases}. \quad (16)$$

For given σ', σ'' and ω, such a point (q', q'') that satisfies Eq. (15) and $\phi(q', q'') < 1$, or Eq. (16) and $\phi(q', q'') > 1$ simultaneously does not always exist. If such a point exists, noting it as (Q', Q''), then $\tilde{f}(\sigma', \sigma'', \omega)$ can be given by the following formula [18]

$$\tilde{f}\left(\sigma', \sigma'', \omega\right) = Q'\sigma' + Q''\sigma'' - \tilde{\tau}\left(Q', Q'', \omega\right). \quad (17)$$

When (Q', Q'') is located in Region I, substituting Eqs. (14) and (15) into (17) and considering Eq. (8), one can get the following multifractal correlation spectrum

$$\tilde{f}(\sigma', \sigma'', \omega) = \omega f[\sigma(Q' + Q'')] + (1 - \omega)\{f[\sigma(Q')] + f[\sigma(Q'')] - D_0\}; \quad (18)$$

while when (Q', Q'') is located in Region II, substituting Eqs. (14) and (16) into (17) and considering Eq. (8), the multifractal correlation spectrum can be expressed as

$$\tilde{f}\left(\sigma', \sigma'', \omega\right) = f\left[\sigma\left(Q'\right)\right] + f\left[\sigma\left(Q''\right)\right] - D_0 - \omega \quad (19)$$

Thus, the expression of $P_\varepsilon(\sigma', \sigma'', d)$ can be obtained.

3. MULTIFRACTAL CORRELATION CHARACTERISTIC ANALYSIS FOR AIRCRAFT ECHOES

This section introduces multifractal correlation theory into the characteristic analysis of real-recorded aircraft echoes from low-resolution radars and takes the echo data from civil and fighter aircraft which are recorded in a VHF-band surveillance radar as the example to perform the analysis. To raise the dependability of target classification, firstly one should do some preprocessing on the raw echo data, such as attitude partitioning (flying towards the radar station, flying in side direction, and flying off the radar station), energy normalizing, so as to diminish the influence of factors such as flying attitude and distance [28].

Because multifractal correlation analysis is to further examine the spatial correlation of two-point singular indexes on basis of multifractal analysis, which means that the data to analyze should have multi-fractal characteristics. Therefore, firstly multifractal analysis should be performed on the investigated echo data to validate their multifractal characteristics. Figures 1 and 2 show the mass index and multifractal spectrum curves of a group of echo data from the two types of aircraft targets; thereinto, the civil and fighter aircraft are flying towards and off the radar station, respectively, and the number of echo data points is 1024. As can be seen from the figures, the echo mass indexes of the two types of aircraft are all convex functions of q, and their echo singular indexes σ also have a certain range of distribution. Therefore, both types of echoes have certain multifractal characteristics. Moreover, the echo multifractal spectrum curves of the two types of aircraft take on right-symmetrically hook-like structure, which indicates that subsets with high probabilities dominate in the echo structure, i.e., components

(a)   (b)
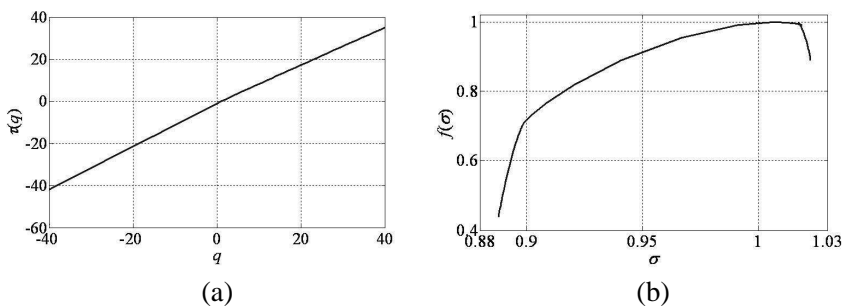
Figure 1. Multifractal characteristics of echoes from civil aircraft. (a) Mass index. (b) Multifractal spectrum.
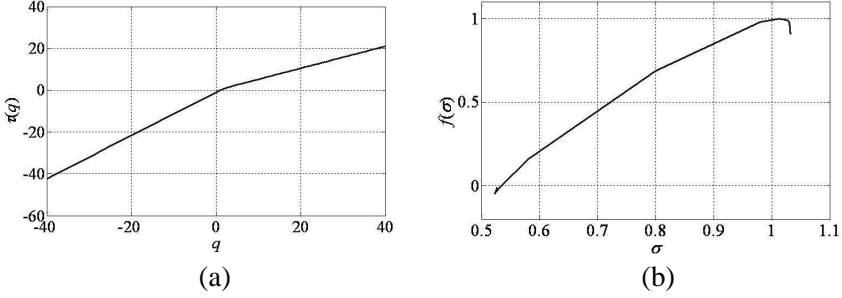
Figure 2. Multifractal characteristics of echoes from fighter aircraft. (a) Mass index. (b) Multifractal spectrum.

with low amplitudes account for a large proportion. In addition, in Figure 2(b), negative values appear in the multifractal spectrum curve, viz., some subsets of σ have negative fractal dimensions, which means that there are some multi-fractal characteristic ripples among different possible samples [29].

Below, the multifractal correlation characteristics of aircraft echoes from surveillance radars will be analyzed. Figures 3 and 4 present 3-D graphs and corresponding contours of $\min\{\phi(q', q''), 1\}$ of the same group of echo data as in Figures 1 and 2. As can be seen from the figures, the whole $q' - q''$ plane can be divided into two regions, i.e., Region I: $\phi(q', q'') < 1$ and Region II: $\phi(q', q'') > 1$, where the corresponding height of the 3-D curved surfaces in Region II are 1; the origin of the $q' - q''$ plane is their saddle points; the $q' = q''$ plane is their plane of symmetry with the corresponding contours symmetrical about the line $q' = q''$ in the $q' - q''$ plane. By Eq. (14), one can figure out the correlation moment exponents of the same group of echo data, as shown in Figure 5, where $\omega = 0.5$. It can be seen from the figure, compared to the moment exponent $\tau(q)$ in the multifractal analysis, the correlation moment exponents $\tilde{\tau}(q', q'', \omega)$ have turned into 3-D surfaces from 2-D curves, and it can be known from Eq. (14) that they can also be divided into two parts corresponding to Regions I and II shown by the contours in Figures 3 and 4.

According to the calculated multifractal spectra, correlation moment exponents along with their relationships with multifractal correlation spectrum shown by Eqs. (15)~(19), one can calculate the corresponding multifractal correlation spectrum with the points in Regions I and II of the $q' - q''$ plane and then put them together to acquire the complete multifractal correlation spectra of aircraft echoes from surveillance radars. Figures 6(a) and (b) show the multifractal
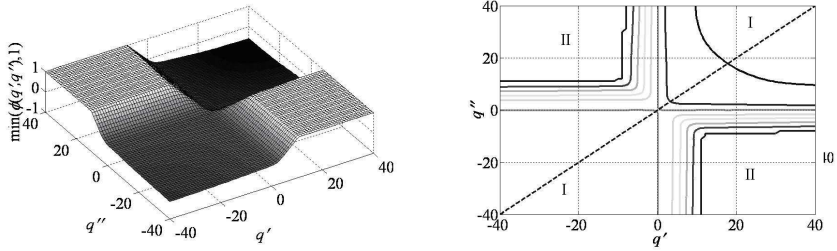
Figure 3. 3-D graph and its contour of $\min\{\phi(q', q''), 1\}$ of echoes from civil aircraft.
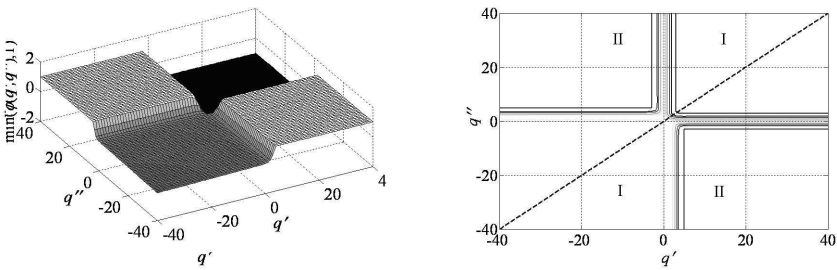

Figure 4. 3-D graph and its contour of $\min\{\phi(q', q''), 1\}$ of echoes from fighter aircraft.

(a)   (b)
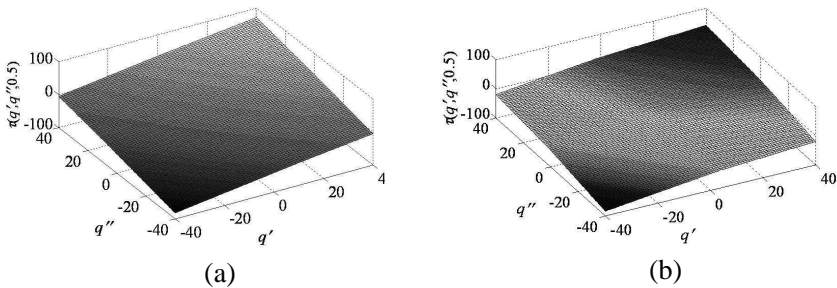
Figure 5. Correlation moment exponents of echoes from two types of aircraft targets. (a) Civil aircraft. (b) Fighter aircraft.

correlation spectra of the same group of echo data from the two types of targets, respectively, as a contrast, Figure 6(c) presents the multifractal correlation spectrum of a group of pure clutter data, and Figures 6(d)∼(f) are their contours in the $\sigma' - \sigma''$ plane respectively. As can be seen from the figures, the multifractal correlation spectra are symmetrical on the $\sigma' = \sigma''$ plane, and there are sudden changes
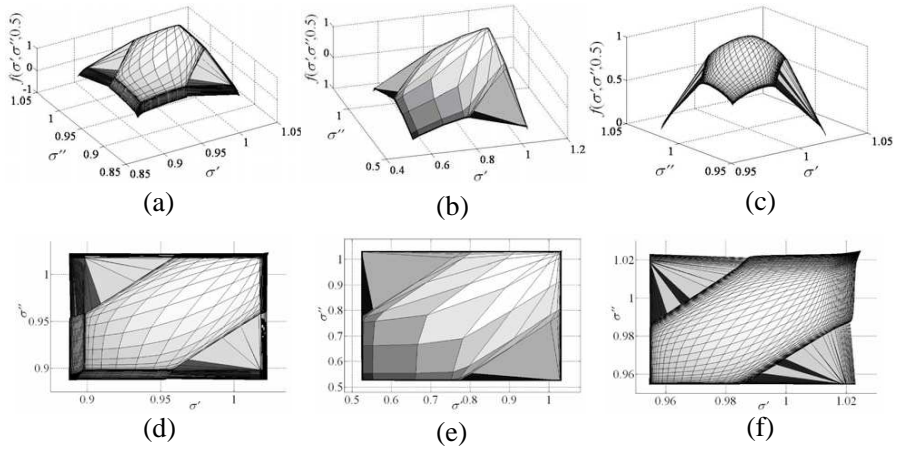
Figure 6. Multifractal correlation spectra as well as their contours in the σ'-σ'' plane, where, (a)$\sim$(c) are the multifractal correlation spectra of echoes from civil aircraft, fighter aircraft and nontarget respectively, and (e)$\sim$(f) are their contours in the σ'-σ'' plane.

from their centers to both wings, which is in accordance with the before-mentioned first order phase transition of the scaling behavior. Moreover, it also can be seen from the figures that the presence of a target broadens the echo multifractal correlation spectrum and shifts the distribution region of the singular index, and the surface texture characteristics have also undergone a significant change. In addition, because different types of aircraft targets have different nonlinear echo modulations due to different physical characteristics, the multifractal correlation spectra of the two types of aircraft targets also show some obvious dissimilarity, which is advantageous for aircraft classification and identification.

4. EXTRACTION OF MULTIFRACTAL CORRELATION SPECTRUM FEATURES

Below, the echo multifractal correlation spectra of different types of aircraft targets will be further analyzed, and their characteristic parameters will be defined. Firstly, according to the characteristic analysis of the echo multifractal correlation spectra of different types of aircraft targets, the following two characteristic descriptive parameters can be defined.

(1) Spectral barycenter

$$\sigma_0 = \frac{\iint \sigma' \left| f\left(\sigma', \sigma'', \omega\right) \right|^2 d\sigma' d\sigma''}{\iint \left| f\left(\sigma', \sigma'', \omega\right) \right|^2 d\sigma' d\sigma''}. \tag{20}$$

As multifractal correlation spectra are symmetrical on the $\sigma' = \sigma''$ plane, the quadrature in Eq. (20) can also be solved on σ'', and the result is the same. Obviously, the point (σ_0, σ_0) describes the distribution barycenter of the multifractal correlation spectrum $f(\sigma', \sigma'', \omega)$ in the σ'-σ'' plane.

(2) Spectral correlation width

$$\sigma_{\text{width}} = \sigma'_{\max} - \sigma'_{\min}, \tag{21}$$

where $\sigma'_{\max}$ and $\sigma'_{\min}$ denote the maximum and minimum of σ', respectively. Similarly, due to the symmetries of multifractal correlation spectra on the $\sigma' = \sigma''$ plane, σ_{width} can also be calculated by the range of σ''. It is easy to know from the definition that σ_{width} depicts the correlation range of singular indexes of $f(\sigma', \sigma'', \omega)$.

Secondly, if taking the slice of $f(\sigma', \sigma'', \omega)$ in the $\sigma' = \sigma''$ plane, one can get a hooked curve shown by Figure 7, which is similar to a multifractal spectrum. If defining the curve asymmetric index

$$R_\sigma = \frac{\Delta\sigma_L - \Delta\sigma_R}{\Delta\sigma_L + \Delta\sigma_R} \tag{22}$$

as another characteristic descriptive parameter for $f(\sigma', \sigma'', \omega)$, where, $\Delta\sigma_L = \sigma_0 - \sigma_{\min}$, $\Delta\sigma_R = \sigma_{\max} - \sigma_0$, and σ_0 is the singular index corresponding to the maximum of the curve, i.e., $\max \tilde{f}(\sigma, \sigma, 0.5)$, then R_σ depicts the asymmetric property of the slice of $f(\sigma', \sigma'', \omega)$ in the $\sigma' = \sigma''$ plane from the whole.

Figure 8 gives the probability density distribution curves of these three multifractal correlation characteristic parameters of radar echoes
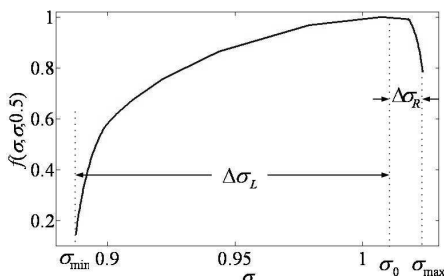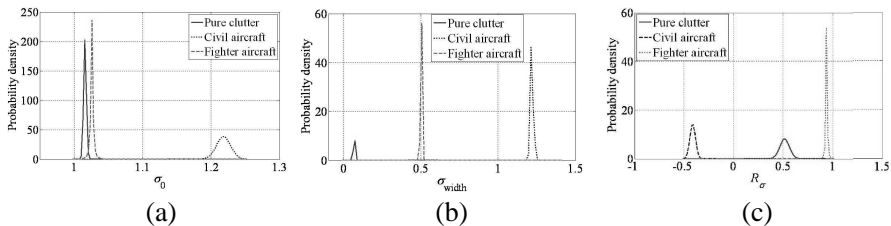

Figure 7. Slice of $f(\sigma', \sigma'', \omega)$ in the $\sigma' = \sigma''$ plane.

Figure 8. Probability density distribution curves of three multifractal correlation characteristic parameters. (a) Spectral barycenter. (b) Spectral correlation width. (c) Asymmetric index.

from a civil aircraft and a fighter aircraft when they fly off the radar station, and as a contrast, those of pure clutter are also presented. As can be seen from the figure, each of the three characteristic parameters has powerful abilities for different types of aircraft targets, and as to the three types of radar echoes, any of the three characteristic parameters can distinguish them easily. Of course, the type of target involved here is less. In the case of many types of aircraft targets needed to identify, these three characteristic parameters can be combined together to identify different types of aircraft targets, so as to obtain a better performance.

5. TARGET CLASSIFICATION EXPERIMENTS

Here the aforementioned real-recorded echo data from six types of aircraft targets will be adopted as the experimental data to do the classification experiments, and the classification method based on multifractal features (CMMF) proposed in [13] will be taken as the contrast to analyze the performance of the classification method based on multifractal correlation features (CMMCF).

   Experiment 1: Take the support vector machine (SVM) [30] as the classifier to analyze the performance of CMMF and CMMCF contrastively when targets fly towards the radar station. In the experiment, the classifier takes the Gaussian kernel $K(x_i, x_j) = \exp(-||x_i - x_j||^2/\sigma^2)$ as the kernel function, and there are three types of targets (Types 1~3) used for the classification experiment, where the numbers of training and testing samples are 1024 and 256, respectively for each type of targets. Because there is no prior knowledge about the parameter σ^2, below, the parameter values which can well classify different types of aircraft targets will be taken as the kernel function parameters. All the correct classification rates (CCRs, here CCR is

defined as the ratio of the number of samples classified correctly to the total number of samples) given in the following are the classification results using the better kernel function parameters. Table 1 shows the CCRs of CMMF and CMMCF. It can be seen from the table that when targets fly towards the radar station, whether for the CCR of each type of aircraft targets or the average CCR, CCRs of CMMCF are all more than ninety-nine percent, which exceed those of CMMF more than four percent.

Experiment 2: Still take SVM using the Gaussian kernel function as the classifier to analyze the performance of CMMF and CMMCF contrastively when targets fly off the radar station. Also there are three types of targets (Type 4~6) used for the classification experiment, and the numbers of training and testing samples are 1024 and 256, respectively, for each type of targets. Table 2 presents the corresponding classification results. As can be seen from the table, when targets fly off the radar station, except for Type 4, the CCRs for the other two types of aircraft targets and the average CCR of CMMCF are all higher than those of CMMF, and the average CCR of CMMCF outstrips that of CMMF more than three percent.

Table 1. Classification results of CMMF and CMMCF when aircraft targets fly towards the radar station.

	CMMF	CMMCF
Type 1	97.20%	100.00%
Type 2	93.43%	100.00%
Type 3	95.08%	99.61%
Average CCR	95.18%	99.87%

Table 2. Classification results of CMMF and CMMCF when aircraft targets fly off the radar station.

	CMMF	CMMCF
Type 4	93.19%	89.51%
Type 5	86.74%	100.00%
Type 6	99.61%	100.00%
Average CCR	92.97%	96.09%

Synthetical analyses of Tables 1 and 2 show that both CMMF and CMMCF have nice classification performance, that their average CCRs are all more than ninety percent, and that CMMCF excels CMMF appreciably in the total performance. The reason is as follows: in comparison with multifractal spectrum, multifractal correlation spectrum further considers the spatial correlation characteristics of singular index, and it can provide more comprehensive self-similar information about a target. In addition, due to having done feature-dimension-reduction-processing, the computation load of CMMCF increases inconspicuously with respect to that of CMMF. Hence, CMMCF is an effective classification method for aircraft targets and deserves applications in engineering practice.

The previous analysis and application of multifractal correlation spectra are all carried out with the assumption that parameter ω equals 0.5. Below, the impact of different values of ω on the classification results will be further analyzed. In Region I, $d \to 1$ when $\omega \to 0$, here Eq. (15) translates into Eq. (16), and thus the phase transition disappears; however, $d \to \varepsilon$ when $\omega \to 1$, here it can be obtained from Eq. (15) that $\tilde{\tau}(q', q'', \omega)$ is dominated by such a point set made up of singular indexes $\sigma(q' + q'')$, i.e., the singular index σ'' of a point found in the small region of σ' equals to σ'. In Region II, $\tilde{\tau}(q', q'', \omega)$ is independently dominated by σ' and σ'' together and independent of ω. Figures 9(a) and (b) present the multifractal correlation spectra when ω equals 0.01 and 0.99, respectively. As can be seen from the figures that when ω is close to 0, the boundaries between Region I and II are already inconspicuous, which are connected into a whole, and the phase transition disappears. When ω is close to 1, the multifractal correlation spectrum is mainly distributed in both wings, i.e., the spectrum is mainly distributed in Region II, and the spectrum in Region I verges on a curve in the $\sigma' = \sigma''$ plane.

(a)   (b)
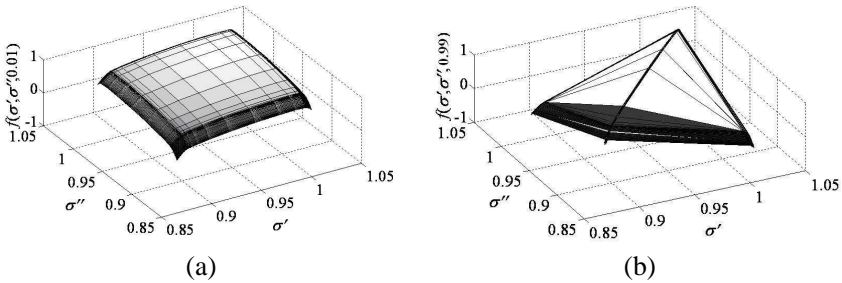
Figure 9. Multifractal correlation spectra of aircraft echoes when ω equals to 0.01 and 0.99 respectively. (a) $\omega = 0.01$. (b) $\omega = 0.99$.

Table 3. CCRs in condition of different ω values.

ω	0	0.25	0.5	0.75	1
Flying towards the radar station	99.22%	99.87%	99.87%	99.87%	99.87%
Flying off the radar station	96.74%	96.88%	96.09%	96.74%	97.00%

To quantify the impact of different values of ω on the classification results, with the same conditions as in Experiment 1 and Experiment 2, target classification experiments are performed again with ω taking different values, respectively. Table 3 gives the average CCRs with ω taking different values when targets fly towards or off the radar station. As can be seen from the table, different values of ω have little effect on the final classification results, which demonstrates that the classification results of SVM have not been affected by the edge transition of the multifractal correlation spectrum caused by the phase transition of the scaling behavior. The main reason is that the difference among echo multifractal correlation spectra of different types of aircraft targets embodies in both scale regions as Regions I and II, and different values of ω just mean redividing these two scale regions. However, the difference among them is still stable. Consequently, the target classification results of CMMCF will not be affected by the parameter ω.

6. CONCLUSIONS

This paper introduces multifractal correlation theory into the echo characteristic analysis and classification of aircraft targets with low-resolution surveillance radars. Firstly, on basis of introducing multifractal correlation theory, the paper analyzes the multifractal correlation characteristics of real-recorded aircraft echo data from a VHF-band surveillance radar. Secondly, based on the previous analysis, it puts forwards the extraction method of multifractal correlation features. Finally, it does target classification experiments using the multifractal correlation features and SVM classifier in condition of no compensation for echo airframe components. The experimental results show that the multifractal-correlation-feature-based SVM classifier can classify different types of aircraft targets effectively, and the proposed method has good classification performance.

ACKNOWLEDGMENT

REFERENCES

1. Huang, P. K., H. C. Yin, and X. J. Xu, *Radar Target Characteristics*, Publishing House of Electronic Industry, Beijing, 2005.

2. Nalecz, M., R. R. Andrianik, and A. Wojtkiewicz, "Micro-Doppler analysis of signal received by FMCW radar," *Proceedings of International Radar Symposium*, 231–235, 2003.

3. Ding, J. and X. Zhang, "Automatic classification of aircraft based on modulation features," *Journal of Tsinghua University (Science and Technology)*, Vol. 43, No. 7, 887–890, 2003.

4. Chen, V. C., F. Y. Li, S. S. Ho, et al., "Micro-Doppler effect in radar: Phenomenon, model, and simulation study," *IEEE Trans. AES*, Vol. 42, No. 1, 2–21, 2006.

5. Zhuang, Z. W., Y. X. Liu, and X. Li, "The achievements of target characteristic with micro-motion," *Acta Electronica Sinica*, Vol. 35, No. 3, 520–525, 2007.

6. Elshafei, M., S. Akhtar, and M. S. Ahmed, "Parametric models for helicopter identification using ANN," *IEEE Transactions on Aerospace and Electronic Systems*, Vol. 36, No. 4, 1242–1252, 2000.

7. Melendez, G. J. and S. B. Kesler, "Spectrum estimation by neural networks and their use for target classification by radar," *Proceedings of International Conference on Acoustics, Speech, and Signal Processing*, 3615–3618, 1995.

8. Moses, R. L. and J. W. Carl, "Autoregressive modeling of radar data with application to target identification," *Proceedings of IEEE National Radar Conference*, 220–224, 1988.

9. Pellegrini, S. P. F. and C. S. Pardini, "Radar signals analysis oriented to target characterization applied to civilian ATC radar," *Proceedings of IEE International Radar Conference*, 438–445, 1992.

10. Chen, F., H. W. Liu, L. Du, et al., "Target classification with low-resolution radar based on dispersion situations of eigenvalue spectra," *Science China: Information Sciences*, Vol. 53, 1446–1460, 2010.

11. Ni, J., S.-Y. Zhang, H.-F. Miao, et al., "Target classification of low-resolution radar based on fractional Brown feature," *Modern Radar*, Vol. 33, No. 6, 46–48, 2011.

12. Li, Q. S., W. X. Xie, and C. Luo, "Identification of aircraft targets based on multifractal spectrum features," *Proceedings of IEEE International Conference on Signal Processing*, 1821–1824, 2012.

13. Li, Q. S. and W. X. Xie, "Target classification with low-resolution surveillance radars based on multifractal features," *Progress In Electromagnetics Research B*, Vol. 45, 291–308, 2012.

14. Li, Q. S. and W. X. Xie, "Multifractal modeling of aircraft echoes from low-resolution radars," *Proceedings of IET International Radar Conference*, 2013.

15. Meneveau, C. and A. Chhabra, "Two-point statistics of multifractal measures," *Physica A*, Vol. 164, No. 3, 564–576, 1990.

16. Lee, S. J. and T. C. Halsey, *Physiea A*, Vol. l64, 575, 1990.

17. O'Neil, J. and C. Meneveau, "Spatial correlation in turbulence: Predications from the multifractal formalism and comparison with experiments," *Physics Fluids A*, Vol. 5, No. 1, 158–172, 1993.

18. Zhou, W., Y.-J. Wang, and Z.-H. Yu, "On the multifractal and multifractal correlation of random binomial measures," *Journal of Nonlinear Dynamics in Science and Technology*, Vol. 8, No. 3, 199–207, 2001.

19. Shadkhoo, S. and G. R. Jafari, "Multifractal detrended cross-correlation analysis of temporal and spatial seismic data," *The European Physical Journal B*, Vol. 72, 679–683, 2009.

20. Hajian, S. and M. S. Movahed, "Multifractal detrended cross-correlation analysis of sunspot numbers and river flow fluctuations," *Physics, Data Analysis, Statistics and Probability*, 1–13, Jul. 2010.

21. Guan, J., N. B. Liu, and J. Song, "Multifractal correlation characteristic for radar detecting low-observable target in sea clutter," *Signal Processing*, Vol. 90, No. 2, 523–535, Elsevier, 2010.

22. Guan, J., N.-B. Liu, J. Zhang, et al., "Multifractal correlation characteristic of real sea clutter and low-observable targets detection," *Journal of Electronics and Information Technology*, Vol. 32, No. 1, 54–61, 2010.

23. Grassberger, P., "Generalized dimensions of strange attractors," *Physics Letters A*, Vol. 97, 227–230, 1983.

24. Halsey, T. C., M. H. Jensen, et al., "Fractal measures and their singularities: The characterization of strange sets," *Physical Review A*, Vol. 33, 1141–1151, 1986.

25. Falconer, K., *Geometry: Mathematical Foundations and Applications*, 2nd edition, 3–108, John Wiley & Sons, England, 2003.

26. Hentschel, H. G. E. and I. Procaccia, "The infinite number of generalized dimensions of fractals and strange attractors," *Physica D*, Vol. 8, 435–444, 1983.

27. Zhang, J., *Fractal,* 2nd edition, Tsinghua University Press, Beijing, 2011.

28. Ji, H., "Research on target recognition and classification method by conventional radar," Doctoral Dissertation of Xidian University, 43–46, 1999.

29. Guan, J., N. Liu, Y. Huang, et al., *Fractal Theory for Radar Target Detectopm as Well as Its Applications,* 149–150, Publishing House of Electronic Industry, Beijing, 2011.

30. Duda, R. O., P. E. Hart, and D. G. Stork, *Pattern Classification,* 2nd edition, Hohn Wiley and Sons, New York, 2001.